



# Modeling and prediction of ventilation methane emissions of U.S. longwall mines using supervised artificial neural networks

C. Özgen Karacan

*National Institute for Occupational Safety and Health, Pittsburgh Research Laboratory, Pittsburgh, PA, 15236, United States*

Received 28 June 2007; received in revised form 8 September 2007; accepted 13 September 2007

---

## Abstract

Methane emissions from a longwall ventilation system are an important indicator of how much methane a particular mine is producing and how much air should be provided to keep the methane levels under statutory limits. Knowing the amount of ventilation methane emission is also important for environmental considerations and for identifying opportunities to capture and utilize the methane for energy production.

Prediction of methane emissions before mining is difficult since it depends on a number of geological, geographical, and operational factors. This study proposes a principle component analysis (PCA) and artificial neural network (ANN)-based approach to predict the ventilation methane emission rates of U.S. longwall mines.

Ventilation emission data obtained from 63 longwall mines in 10 states for the years between 1985 and 2005 were combined with corresponding coalbed properties, geographical information, and longwall operation parameters. The compiled database resulted in 17 parameters that potentially impacted emissions. PCA was used to determine those variables that most influenced ventilation emissions and were considered for further predictive modeling using ANN. Different combinations of variables in the data set and network structures were used for network training and testing to achieve minimum mean square errors and high correlations between measurements and predictions. The resultant ANN model using nine main input variables was superior to multilinear and second-order non-linear models for predicting the new data. The ANN model predicted methane emissions with high accuracy. It is concluded that the model can be used as a predictive tool since it includes those factors that influence longwall ventilation emission rates.

© 2007 Published by Elsevier B.V.

*Keywords:* Longwall mining; Ventilation; Methane emissions; Principle component analysis; Artificial neural networks

---

## 1. Introduction

Longwall mining is an underground mining method that can maximize coal production in coalbeds that contain few geological discontinuities. In these operations, a mechanical shearer progressively mines a large block of coal, called a panel, which is outlined with development entries or gate roads. This is a continuous

process in an extensive area, where the roof is supported only temporarily during mining with hydraulic supports that protect the workers and the face equipment (Fig. 1). As the coal is extracted, the supports automatically advance and the roof strata are allowed to cave behind the supports (Karacan et al., 2007a).

Methane emissions can adversely affect the safety of underground coal miners. During longwall mining, methane emissions can originate from three major sources. These sources are: 1) gas emissions from the

---

*E-mail address:* [cok6@cdc.gov](mailto:cok6@cdc.gov).

ribs surrounding the bleeder ventilation system, 2) gas emissions from the active longwall face and mined coal on the conveyor belts, and 3) gas emissions from subsided strata (Mucho et al., 2000).

The first gas source originates from the unmined coalbed adjacent to the development entries of the bleeder system and from the solid coal ribs. Although this emission tends to decrease over time, its total may become a significant contributor of gas to the bleeder ventilation system over time (Mucho et al., 2000). The second source is the combination of the gas content from the mined coal itself, the methane being emitted from the fresh face on the longwall, and the methane emitted from the coal transported out of the mine by the conveyor belts. Methane emissions from the face, ribs, and conveyor belt are directly discharged into the mine ventilation air; therefore, the ventilation system must have sufficient capacity to maintain methane levels within statutory limits. The third source is the fractured and caved rock in the subsided strata (gob) overlying the extracted panel as the longwall face advances. The subsided strata are generally characterized as being made up of the caved zone, fractured zone, and the bending zone. The caved zone is characterized as a fragmented rock mass (completely caved) overlain by strata with extensive fractures (partially caved). The height of the caved zone is about 3 to 6 times the thickness of the mined coalbed (Singh and Kendorski, 1981; Palchik, 2003). The stress relief due to caving causes the overburden strata above the caved zone, including gas-bearing coalbeds, to fracture both vertically and horizontally. The thickness of the fractured zone can vary up to 100 times the height of the mined coalbed, depending on the size of the panel, the geology, and the geomechanical properties of the layers (Palchik, 2003). The methane from this source is usually controlled by vertical boreholes drilled into the fractured zone to reduce the migration of methane from the fractured zone to the caved zone and finally to the ventilation system.

Accurate prediction of longwall methane emissions is important so that adequate ventilation air is supplied to dilute and render harmless high gas levels that threaten mine safety. It is also important to identify opportunities to utilize mine ventilation air for energy production. Underground coal mines worldwide liberate an estimated  $1\text{--}1.5 \times 10^{12}$  scf ( $29\text{--}41 \times 10^9$  m<sup>3</sup>) of methane annually, of which less than  $2.3 \times 10^9$  m<sup>3</sup> ( $81 \times 10^9$  scf) are used for fuel (Bibler et al., 1998). Thus, in order to provide a safer mining environment to underground miners and to make investment decisions into methane utilization technologies, ventilation emissions of the longwall mines must be predicted accurately.

Accurate prediction of the rate of methane flow into the working areas and eventually into the ventilation system is complex due to the large number of variables involved with these potential emission sources. Some of the variables reported by Lunarzewski (1998) are lithology- and stratigraphy-related and include coal and rock properties in the floor and roof strata, depth of the mined coalbed, reservoir properties of coalbed, gas content of mined coal seams, coal rank, and strength of the overlying strata. Variables originating from the mining process include longwall face width, face advance rates, methane drainage, conveyor speeds, and thickness of the mined seam, as well as time-dependent changes in these parameters.

The complexity of the longwall mining process and its associated methane sources have been modeled by several researchers. Schatzel et al. (2006) and Krog et al. (2006) empirically determined the increase in emissions for wider longwall faces using a graphical method and by including the effects of various methane contributors, respectively. Also, by the premise that gas emissions in underground mine environments can be linked to different stages in the life of a coal mine, the following empirical model was suggested (Lunarzewski, 1998):

$$Q(y) = \frac{g}{CA} \left( \left( \sum_0^{y+1} C \right)^m + 1 - \left( \sum_0^y C \right)^m + 1 \right) \quad (1)$$

where:  $Q(y)$  is the average methane emission in a year 'y' of the mine's existence (m<sup>3</sup>), CA is the coal production in the most recent year only (tonnes), C is the coal production for the life of the mine up to year 'y' (tonnes), and g and m are the site-specific coefficients dependent upon geological and mining conditions. In other words, this approach summarizes methane emissions as a function of coal production only and lumps other variables into empirical constants. A similar, lumped-parameter approach for estimating the instantaneous volume of gas released from all potential sources is given by Lunarzewski (1998):

$$R = a\sqrt{CP} + b \quad (2)$$

In this equation, R is the total methane emission rate (liters per second), CP is the daily coal production rate (tonnes), and a and b are empirical constants related to coal production levels and number of working days per week.

Although simple to use, the above approaches are site-specific and require a long period of data collection before a correlation can be established for predictions. Also, they lump the variables into two empirical

constants which limits their applicability for other mines with similar coal production levels but different mining or geological conditions.

Some of the limitations of empirical models can be addressed by calibrating the models and realistically representing additional variables. Lunarzewski (1998) used boundary element and sequential bed separation to model floor and roof strata relaxation and immediate roof bending separation. “Floorgas” and “Roofgas” simulation programs were developed to characterize the strata relaxation zones, gas emission boundaries, and parameters for gas emission prediction. Tomita et al. (2003) developed a three-dimensional (3-D) finite element model (FEM) to predict the volume of methane gas emitted from surrounding coal and rock layers based on stress distribution and permeability changes. Karacan et al. (2005, 2007b) developed a 3-D reservoir model of a longwall mining district to simulate the effects of increasing longwall panel widths on methane emissions, the performances of gob gas ventholes, and degasification planning. This work predicted an increase in emissions due to increasing panel width and the optimal gob gas completion and placement strategies used to prevent the gas from entering the underground workplace. However, numerical models require expertise in users and, in most cases, specialized and expensive software packages. Also, it is not possible or feasible to numerically represent every process that contributes to mine emissions with these models.

Artificial neural networks (ANNs), on the other hand, are adaptable systems that can determine relationships between different sets of data. ANNs have been developed to solve problems where conventional computer models are inefficient. These problems are either the non-polynomial type, having no polynomial relationship, or very complex problems that are difficult to describe mathematically. The key advantages of neural networks are their abilities to learn, to recognize patterns between input and output space, and to generalize solutions. Statistical techniques such as multiple regression analysis have been used widely for these kinds of problems, but they often fail in accuracy of prediction, especially in the face of highly non-linear relationships.

ANNs, due to their flexibility, have found their way into many fields of application. Patel et al. (2007) used artificial neural networks for estimation of gross calorific values of coals. Bagherieh et al. (in press) used the technique to study the relationships between petrography and grindability of Kentucky coals. Yilmaz et al. (2002) used ANN and fractal geostatistics to solve the optimum bit selection problem during drilling in a

carbonate field. Sousa et al. (2007) performed a study to predict atmospheric ozone concentrations using principle component analysis and ANN. Karacan (in press) integrated reservoir simulations during development mining with ANN to predict methane emissions into roadways and to optimize ventilation air requirements. Maier and Dandy (2000) provided an overview of modeling issues and application of ANN for forecasting water resources.

The aim of this paper is to develop an ANN-based methodology to predict ventilation emissions from longwall mines for mine safety applications and to identify opportunities for utilizing ventilation methane. Ventilation emission data obtained from different U.S. mining regions were combined with corresponding coalbed properties, geographical information, longwall operation parameters, and productivities. The database was analyzed using PCA to reduce complexity and to determine the variables to be considered for ANN modeling. The ANN model was built using a multilayer perceptron (MLP) approach and was trained and tested using the database to achieve minimum mean square error and high correlations between measurements and predictions.

## 2. Description and analysis of database

### 2.1. Sources of input data for ventilation emission modeling

In developing the database for modeling ventilation emissions, 63 longwall mines in 10 states operating between 1985 and 2005 were analyzed. Available data sources were searched and evaluated carefully for these mines to extract important parameters relevant to ventilation emissions. These sources provided gas contents of the mined coalbeds, annual coal productions and emissions, longwall operational parameters, and mine characteristics.

Gas contents of the mined coalbeds, based on their geographical location at the mining depths, were compiled from a report published by Diamond et al. (1986). The publication contains approximately 1500 coal samples taken during various drilling operations from more than 250 coalbeds in 17 states. The components of total gas content (lost, desorbed, and residual gas contents) were reported along with sample location (state and county), sample depth, coalbed name, coal rank, and ash content. The lost gas was determined by a graphical method which estimated how much gas was lost during core recovery. Desorbed gas was determined using the direct method determination

of gas content (Diamond and Schatzel, 1998) and residual gas was determined after crushing the coal samples using a ball mill. The total gas content was reported as the sum of all three components.

Annual coal production and ventilation emission data of longwall mines included in this study were taken from the U.S. Environmental Protection Agency (EPA) reports (1994, 1997, 2005) published to identify coal mine methane production opportunities in U.S. coal mines. These reports list various general mine information including geographical data, availability of degasification systems, sulphur content, and heating value of mined coals along with annual coal productions and emissions from ventilation systems. The reports contain information for both large room-and-pillar and longwall operations. (However, in this study, only longwall mines

were considered for analysis.) In the EPA reports, most of the profiled mines are large operations with coal productions exceeding one million tons per year. Coal production data reported in EPA reports were primarily based on the U.S. Energy Information Administration (EIA) database, which is supplemented with data from coal producing states and from the U.S. Mine Safety and Health Administration (MSHA). The data for 2004 and 2005 were taken directly from MSHA's data retrieval system (MSHA, 2007). Emissions data from the ventilation systems were collected by MSHA personnel, who measured methane emission rates at each coal mine on a quarterly basis. Measurements were performed underground at the same locations each time. The reported ventilation emissions for a given year are averages of the four quarterly tests.

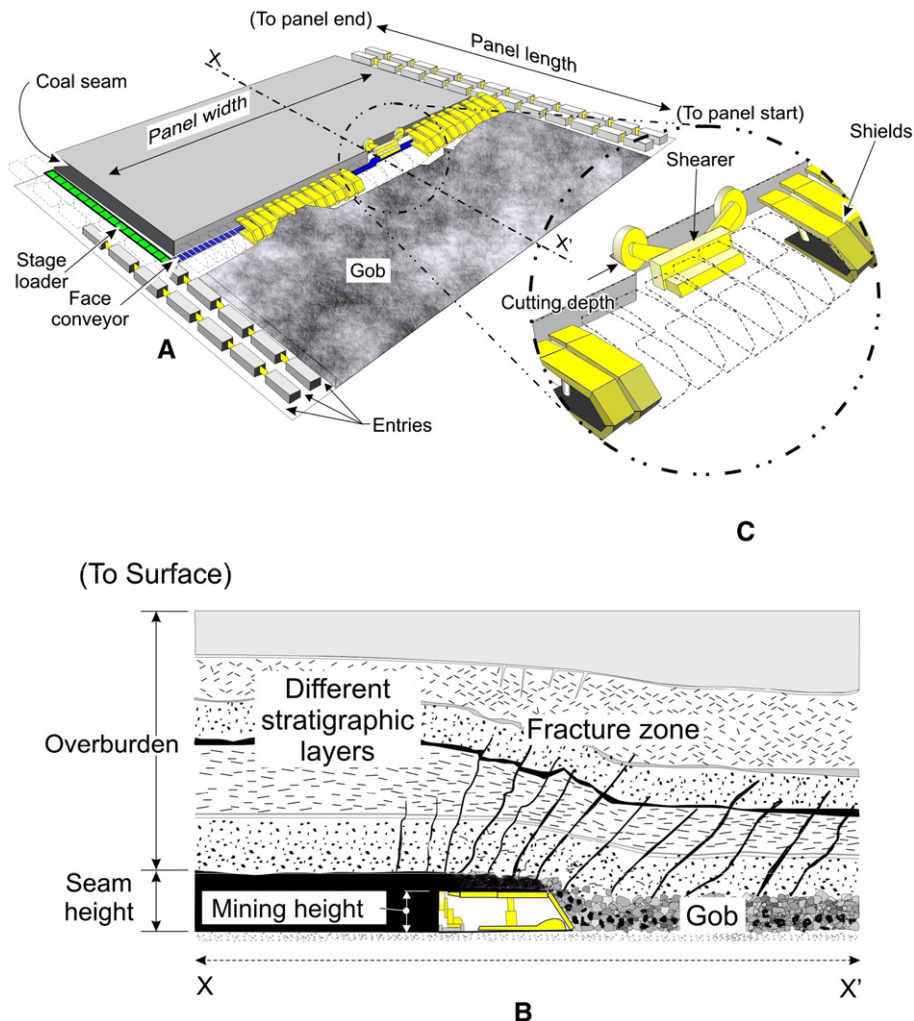


Fig. 1. Schematic representations of a panel surrounded with a three-entry gateroad system (A). B is a vertical cross-section along the X–X<sup>1</sup> profile in A. C is a detailed view of shearer and cutting depth while mining coal.

Table 1

The number of mines and the mine names in each state included in the methane emission database

State		No. of mines	Mine names
Alabama	AL	8	Blue Creek No.3, Blue Creek No.4, Blue Creek No.5, Blue Creek No.7, North River, Mary Lee, Oak Grove, Shoal Creek
Colorado	CO	4	Deserado, Dutch Creek, Golden Eagle, West Elk
Illinois	IL	7	Galatia, Old Ben 24, Old Ben 25, Old Ben 26, Orient No.6, Monterey No.1, Rend Lake
Kentucky	KY	4	Wolf Creek No. 4, Wheatcroft No. 9, Camp No.11, Baker
Maryland	MD	1	Mettiki
Ohio	OH	4	Meigs No. 2, Meigs No. 31, Powhatan No.4, Powhatan No.6
Pennsylvania	PA	10	Bailey, Eighty Four, Enlow Fork, Maple Creek, Cambria, Cumberland, Warwick, Homer City, Dilworth, Emerald
Utah	UT	4	Aberdeen, Sunnyside No. 1, Dugout Canyon, West Ridge
Virginia	VA	7	Buchanan, V. P. No.8, V. P. No.1, V. P. No.6, V. P. No.5, V. P. No.3, McClure No. 1
West Virginia	WV	14	Blacksville No.2, Federal No.2, Loveridge No. 22, McElroy, Pinnacle No. 50, Robinson Run No. 95, Ireland, Osage No. 3, Shoemaker, Windsor, Shawnee, Arkwright, Blacksville No.1, Humphrey No.7

Mining parameters and mine characteristics affect how much and how fast methane will be generated as a result of coal production. These factors also affect how much strata gas will be released and how much of it will enter the ventilation system as a result of caving and fracturing of the overlying strata. The annual data representing mine characteristics and mining parameters were compiled from 1985–2005 issues of Coal Age (Mining Media Inc.), which publishes longwall census data annually. The tabulated data for each operation in the corresponding year includes seam height, cutting height, cutting depth, overburden thickness, longwall panel width, longwall panel length, number of development entries, face conveyor speed, and stage loader speed.

Table 1 shows the number of longwall operations in each state. Table 2 lists variables and their units. There were some important considerations when preparing the final database. One of them was the need to form a complete set of input data using each source for a particular mine and year. For instance, if the production and emission data were available for a particular mine and

year, but the census data were not, then that year's entry was excluded from the database. Also, the operating status and, sometimes, the names of the mines had changed over the 20-year period. Some of the mines producing coal in 1980s were abandoned, while new ones were started in later years. After evaluation of all data, the database used for ANN modeling consisted of 538 data entries with 24 variables spanning a 20-year period (Table 2).

## 2.2. Discussion of database parameters for their potential effects on ventilation emissions

This section summarizes the possible effects on ventilation emissions of the variables presented in Table 2.

Table 2

The variables and their units in the database for each mine compiled from different sources

Variable	Unit	Minimum	Maximum	Mean	Std. dev.
State	–				
Basin	–				
<b>County</b>	–				
<b>City</b>	–				
Degasification	Yes/No				
<b>Mined</b>	–				
<b>coalbed</b>					
<b>Sulphur amount</b>	%				
<b>Coal calorific value</b>	BTU/lb				
Lost+ desorbed gas	scf/ton	6.4	542.1	176.5	144.0
Residual gas	scf/ton	3.2	97.4	47.8	29.3
Total gas	scf/ton	9.6	585.9	224.3	135.7
Rank	–				
<b>Ash content</b>	%				
Coal production	10 <sup>6</sup> short ton/y	0.1	11.1	3.3	2.1
Seam height	inch	39.0	276.0	80.2	34.3
Cut height	inch	43.0	156.0	77.7	18.7
Panel width	ft	400.0	1100.0	823.6	149.5
Panel length	ft	2200.0	13000.0	7679.3	2361.8
Overburden	ft	300.0	2700.0	994.3	509.0
Number of development entries	–	2.0	5.0	3.5	0.6
Cut depth	inch	27.0	44.0	34.7	4.4
Face conveyor speed	ft/min	187.0	450.0	278.1	41.5
Stage loader speed	ft/min	220.0	600.0	353.7	64.3
<b>Year</b>	–				

Variables in bold were excluded from further analysis. Table also shows the ranges of *numeric* input data included in the PCA analysis. Alphanumeric data were represented in the PCA analysis by assigning codes. (SI conversions: 1 inch=0.0254 m, 1 ft=0.3048 m, 1 ft<sup>3</sup>=0.02832 m<sup>3</sup>).

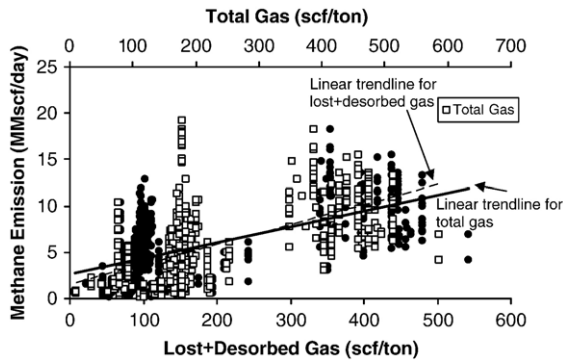


Fig. 2. Methane emissions from ventilation system of the mines from 1985 to 2005 as a function of total and lost plus desorbed gas contents of the coalbeds they operated ( $1 \text{ ft}^3 = 0.02832 \text{ m}^3$ ,  $1 \text{ MMscf} = 28,320 \text{ m}^3$ ).

Fig. 1 provides schematic representation of some of the variables discussed in the following sections. Fig. 1A shows the graphical representation of a panel surrounded with a three-entry gateroad system, the gob and caving behind the shields, and the face area, conveyors, and unmined section of the coal seam. Fig. 1B is a vertical cross-section along the X–X<sup>I</sup> profile in Fig. 1A. This figure shows how overlying strata are supported by shields above the personnel and shearer, the caving and fracturing of the overlying strata after the longwall supports advance, the coal seam, and mining heights. Fig. 1C is a detailed view of shearer and cutting depth while mining coal.

### 2.2.1. Parameters related to gas content of the coal seam

Gas content is among the key data included in coalbed methane resource estimations (Boyer and Qingzhao, 1998). The gas content data, when combined with geologic and engineering data, can be used as a basis for an initial estimate of methane emissions and ventilation requirements (Diamond et al., 1986; Noack, 1998; Karacan and Diamond, 2006).

Gas content has three major components: lost gas, desorbed gas, and residual gas. The combination of all of these gives the total gas content of the coalbed. During mining, all three components potentially contribute to methane emissions into the mine atmosphere, and these emissions can increase as the gas content of the coal increases. Fig. 2 shows the change in ventilation emissions from the mines in the database versus lost plus desorbed and total gas contents of the mined coal seams. The figure shows that there is a general positive correlation and that emissions tend to increase with increasing gas contents.

Rank represents the level of maturation reached in a coal seam and usually increases with increasing depth. Most longwalls, as well as most commercial coalbed methane projects, operate in bituminous coalbeds. The coals of sub-bituminous to low-volatile bituminous range usually provide high gas content and natural permeability (Steidl, 1996). Mining coals of this rank, particularly medium- to low-volatile bituminous coals, potentially liberates high amounts of gas into the ventilation system.

Depth of the mined coal seam, or its overburden (Fig. 1B), impacts methane emissions in two ways. First, for coals of the same rank, gas content generally increases with increasing depth (Kim, 1977). The second impact of overburden is on the disturbance created in the overlying strata. This effect can be relative to the width of the extracted panel. If panel width (Fig. 1A) is greater than overburden depth, the panel is referred as a “supercritical” panel (Mucho et al., 2000). This designation implies that, for the same type of roof material and stratigraphic sequence, the caving will be more complete after mining compared to a situation where the panel width is less than the overburden depth. Besides its ground control implications, this situation may potentially affect the methane reservoir and permeability pathways in the overlying strata and may impact the emissions into the mine and into the ventilation system (Karacan et al., 2005, 2007a). Fig. 3 shows ventilation emissions of the mines in the database of this study versus overburden thickness of the mined coal seams. The plot shows that there is a general positive correlation between methane emissions and overburden depth.

### 2.2.2. Panel size, coal productivity, and longwall operational parameters

Panel dimensions influence ventilation emissions by impacting the dimensions of the subsided strata

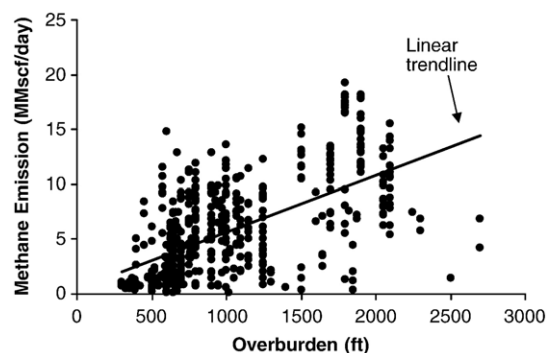


Fig. 3. Methane emissions from ventilation system as a function of overburden thicknesses from 1985 to 2005 ( $1 \text{ ft} = 0.3048 \text{ m}$ ,  $1 \text{ MMscf} = 28,320 \text{ m}^3$ ).

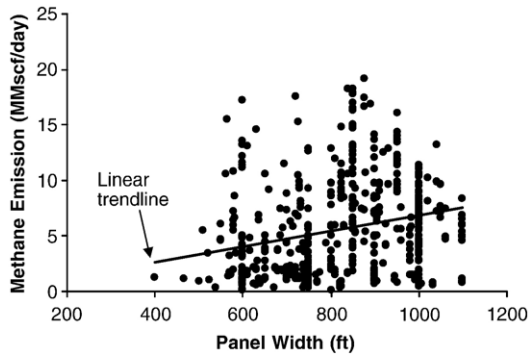


Fig. 4. Methane emissions from ventilation system as a function of longwall panel widths of the analyzed mines between 1985 and 2005 (1 ft=0.3048 m, 1 MMscf=28,320 m<sup>3</sup>).

overlying the extracted panel and the emissions from the longwall face. Current panels are typically 305 m (1000 ft) in width (with a continual trend towards even wider panels) and usually over 3000 m (10,000 ft) in length. The increasing size of longwall panels, while helping to increase coal production, may also increase methane emissions due to the exposure of the mining environment to a larger area of fractured, gas-bearing strata. If not captured effectively, additional gas emissions from bigger, fractured formations (Fig. 1B) enter the mining environment and increase ventilation emissions (Karacan et al., 2005). The increase in panel width (Fig. 1A) also increases face emission rates during mining operations. This gas inevitably enters the ventilation system (Schatzel et al., 2006; Krog et al., 2006).

Fig. 4 shows a plot of ventilation emissions of the longwalls in the database as a function of their face widths. The linear trendline passing through the data shows that there is a slight positive correlation between ventilation emissions and longwall face widths. However, since ventilation emission is affected by other mining and geological related factors too, this relation is far from being a strong linear one.

Cut depth (Fig. 1C) is the slice of coalbed that is mined by the shearer during each pass. In general, the greater the cutting depth, the more coal is produced per rotation and the greater the emissions. However, emissions may also be affected by the rotational speed of the cutting drum and the loading rate of the shearer. If the drum is rotating fast compared to haulage speed, then a finer coal fraction is produced (Peng, 2006), which potentially increases emissions.

The face conveyor and stage loader (Fig. 1A) are parts of the coal transfer system. Their main roles are to carry the cut coal from the face environment and to

transfer it to the belt conveyor, respectively. They should have high capacity and should operate as fast as is practical to ensure continued coal production. Their speeds are important so that the coal is moved from the face area as quickly as possible to minimize emissions from the broken coal on the conveyor.

Most of the operational parameters contributing to gas emissions also impact coal production. Practical experience has shown that gas emissions are directly related to coal production (Lunarzewski, 1998). The more coal that is mined the higher the emission rates. Fig. 5 shows the relationship between coal productivity of the mines in the database and their methane emission rates as measured in the ventilation system. The figure shows that emissions are positively correlated with coal production.

### 2.2.3. Seam and cut (mining) height

Although mining height is an operational parameter, it is usually equal or related to the seam height. Usually, mining height is equal to the seam height. In some thin seam mines, the roof is also extracted, depending on the rock material, to make room for equipment and personnel. Seam and mining height impact ventilation emissions because thick, permeable, and gassy coalbeds potentially generate more gas from the longwall face compared to their thinner counterparts. In addition, caving height is proportional to mining height (Peng, 2006). Thus, the greater the mining height, the higher the caving will be and the greater the potential for more gas to flow into the gob from the overlying strata. If the mining height is less than the coal seam height—for example in thick seam mining by top coal caving (Ünver and Yasitli, 2006) or where the operator leaves top or bottom coal for ground control purposes—some of the unmined coal seam stays in the gob and may generate additional gas.

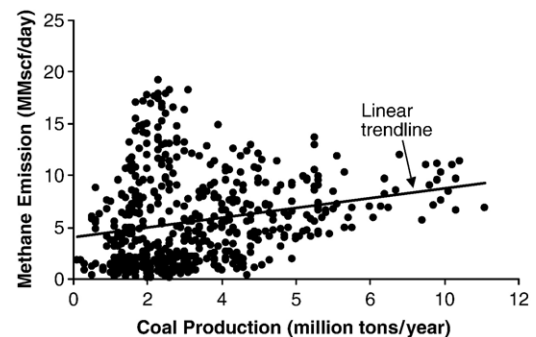


Fig. 5. Methane emissions from ventilation system as a function of annual coal productions of the analyzed mines between 1985 and 2005 (1 MMscf=28,320 m<sup>3</sup>).

#### 2.2.4. Parameters related to gas removal

Gateroads are an integral part of longwall mining. They are mainly used for ventilation and transportation pathways in underground operations. In the U.S., some of the early mines used five-entry gateroads. Today, three-entries are preferred since they require less development footage compared to four- or five-entry systems. A four-entry system is used in coal seams of low height and high gas content. These mines require more air and thus more entries to minimize resistances. Two-entry gateroads require a special variance and are used in deep mines with a thick layer of strong overlying strata, such as operations in Colorado and Utah (Peng, 2006). Thus, the increased number of entries is both an indicator of the gassiness of the mine and a contributor to emissions since it creates additional surfaces from which methane can flow into the ventilation system.

Degasification of the coal seam and the overlying strata prior to and during mining are effective ways of controlling methane emissions during mining (Thakur and Puondstone, 1980; Diamond, 1994; Karacan et al., 2007b). An effective degasification process can reduce emissions into the ventilation system. Depending on the gassiness of the coal seam and the fractured strata, horizontal boreholes, vertical boreholes, or gob gas ventholes can be used. The number of boreholes, their locations, and their degasification durations may change based on site-specific factors (Diamond, 1994).

#### 2.2.5. Geographical location (state and basin)

A strong relationship exists between gas emission rates and geological factors, such as stratigraphy and the gas contents and strengths of the overlying and underlying strata. Pashin (1998) reported, based on investigations in the Black Warrior Basin and in the San Juan Basin, that regional variations in sequence stratigraphy were useful for characterization of coalbed methane reservoirs, in that they were affected by regional sedimentology and tectonics. Although geographical location is not directly related to methane emissions, it indirectly identifies the differences in underground stratigraphy (schematically shown in Fig. 1B) between different locations. This variable also may be used to identify geological differences in the absence of direct geological data.

The discussions in this section show that complex relations exist between different factors and the resultant emission rates from longwall operations. In fact, these relations are too complex to be explained by simple polynomial relations or statistical methods, suggesting that an ANN approach may be a good candidate for modeling ventilation emissions.

### 3. Model complexity reduction for ANN development: Principle component analysis (PCA)

As in any other prediction models, in ANN modeling, the number and selection of appropriate input parameters are very important (Faraway and Chatfield, 1998). Thus, the key issue is to determine and select the appropriate input parameters based on knowledge of the causal variables and a familiarity with the modeled system.

Hybrid ANN models integrated with various statistical techniques partially address the need for reducing the number of input parameters by internally determining which model inputs are critical among all variables for a modeling study. One of the disadvantages of hybrid models is that presenting a large number of inputs to ANN models, while relying on the network to determine the critical model inputs, usually increases network size and decreases processing speed (Maier and Dandy, 2000). Although easier to implement especially when the modeled system is not well understood, these models select variables automatically and thus eliminate the knowledge and expertise of the user in selecting the inputs. Therefore, if the relationship to be modeled is well understood, there are distinct advantages in using analytical techniques such as cross correlation analysis or principle component analysis (PCA) to determine the inputs for ANN models (Maier and Dandy, 2000).

In this study, PCA was used for selecting the most appropriate input variables from all the variables presented in Table 2. Identifying principle components (PCs) reduces the dimensionality of a data set, while retaining as much of the variance in the data set as possible. This reduction is achieved by transforming the original variables into PCs, which are orthogonal and highly uncorrelated to each other. Most of the variance in the data set is retained in the first components that contribute to variance to a greater degree. Elimination of PCs that do not contribute to the variance of the data decreases the dimension of the data set, while revealing information on correlations between variables and their weights in corresponding PCs (Davis, 1986; Grima, 2000; Grima et al., 2000).

#### 3.1. Preliminary data evaluations and results of PCA

Before performing PCA using XLStat statistical package (Addinsoft, 2007), all the variables in Table 2 were evaluated. The variables of city, county, coalbed name, calorific value of the produced coals, ash contents, and sulphur contents were eliminated. This was done because these variables were more related to

Table 3

Eigenvalues and the variances explained by principle components extracted using 538 observations of 17 variables shown in Table 2

PC	Eigenvalue	Variance (%)	Cumulative %
1	4.62	27.18	27.18
2	3.88	22.84	50.02
3	2.42	14.26	64.28
4	1.49	8.77	73.05
5	0.92	5.41	78.46
6	0.64	3.75	82.21
7	0.62	3.65	85.86
8	0.53	3.11	88.97
9	0.43	2.56	91.52
10	0.41	2.43	93.95
11	0.31	1.81	95.76
12	0.27	1.58	97.34
13	0.19	1.10	98.45
14	0.13	0.76	99.20
15	0.11	0.65	99.85
16	0.03	0.15	100.00

The first five PCs represent ~80% of the total variance.

combustion efficiency rather than their methane emission potentials, or they were represented by other parameters in the data set. The variable “year” is categorical information and cannot be used as a variable for future projects or for new operation conditions to predict emissions. Thus, this parameter was also eliminated from the data set. With elimination of these seven variables, Table 2 was reduced to 17 variables to perform PCA. The variables represented by alphanumeric information in this table were designated by numeric information for PCA. The presence or absence of any degasification system in a particular mine was labeled either 1 or 0, respectively, in order to be included in the PCA. Table 2 also gives the ranges and mean and standard deviation information for the inputs represented by numeric information.

Table 3 lists the results of the principle component analysis performed on the remaining 17 variables in Table 2. It can be seen that all variance in the data is represented by 16 PCs. However, approximately 80% of the total variance in the data can be represented by the first five PCs. The individual contributions of the remaining 11 PCs are small and their total contribution is only 20% of the total variance. Table 3 also lists the eigenvalues, which show the proportion by which an eigenvector’s magnitude is changed. The eigenvectors with the largest eigenvalues represent the dimensions with the strongest correlation in the data set. This data set shows that the highest correlations are also in the first five PCs. Thus, the first five PCs were selected for the principle component matrix. Table 4 shows the loadings, which indicates the influence of the variables in these

five PCs. Positive loadings indicate positive correlations, whereas negative loadings indicate negative correlations. Also, loadings close to 1 indicate stronger correlations.

Fig. 6 shows the correlation circle for the factor loadings of the first two components. In this plot, if any two variables are far from the center and if they are close to each other, it indicates that they are significantly and positively correlated. If any two variables are orthogonal, then there is no correlation between them. On the other hand, if they are on the opposite sides of the center, then they are negatively correlated. When the variables are close to the center, it means that some information may be carried over to other axes (Addinsoft, 2007). Fig. 6 shows that gas content and rank of the coal are correlated with overburden thickness and that they are significant for the first PC. Likewise, mine operation parameters and panel width are correlated and they are significant for the second PC. On the other hand, seam height and cut height are close to the center, suggesting that their information can be better represented by other axes.

Fig. 7 shows a two-dimensional map of the factor scores of each mine on the first and second PC axes. This plot enables analysis of the trends and groupings between observations. There are two major clusters, one formed by Virginia and Alabama mines and the other one formed by the mines in the remaining eight states in varying locations. Virginia and Alabama mines are separated from the others because of their mining depths, gassiness, and operational parameters. There are

Table 4

Loadings of the variables in the principle component matrix for the first five principle components

Variables	PC 1	PC 2	PC 3	PC 4	PC 5
Degasification	0.422	0.411	0.288	0.318	0.343
Basin	-0.710	0.103	0.476	0.376	-0.285
State	-0.479	0.227	0.683	0.371	-0.249
Seam height	0.251	0.223	-0.613	0.628	0.035
Cut height	0.316	0.058	-0.662	0.581	0.082
Panel width	-0.071	0.755	-0.133	-0.214	0.011
Panel length	-0.372	0.600	-0.015	-0.302	0.122
Overburden	0.790	0.099	0.217	0.101	-0.098
Number of entries	0.347	-0.102	0.521	-0.038	0.635
Cut depth	0.002	0.755	-0.151	-0.058	-0.065
Face conveyor speed	-0.049	0.838	-0.104	-0.122	-0.172
Stage loader speed	0.073	0.800	-0.110	-0.166	0.116
Lost+desorbed gas	0.900	0.198	0.198	0.004	-0.246
Residual gas	-0.520	0.359	0.436	0.408	0.245
Total gas	0.843	0.287	0.305	0.093	-0.209
Rank	0.853	0.186	0.349	-0.090	-0.068
Coal production	-0.361	0.671	-0.098	0.035	0.088

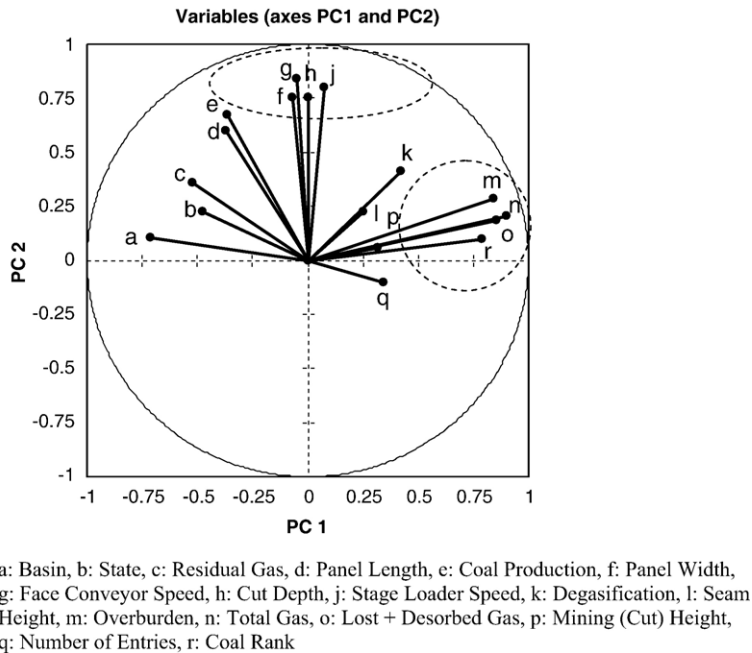


Fig. 6. A correlation circle showing the magnitude and directions of the variable loadings in the first two principle components.

also some scattered data points between these two main clusters. These are due to operations having characteristics similar to those in either cluster. For instance, the data points between the clusters located on the positive side of the PC2 axis belong to Pinnacle No. 50 mine. Although this mine is geographically located in West Virginia, it operates in the Pocahontas No. 3 coalbed, making it similar to the Virginia mines. Similarly, some of the data on the negative side of the second PC axis belong to North River mine of Alabama. However, its

operating depth is shallower [152 m–183 m (500–600 ft)] and the gas content of this coalbed is less compared to the other Alabama mines. Thus, it is separated from the group and approaches those operations with which it shares similar characteristics.

### 3.2. Analysis of rotated principle component matrix

In order to improve interpretability, PCA was continued with a new component matrix that was created by using Kaiser's varimax rotation method, in which PC axes are rotated to a position in which the sum of the variances of the loadings is a maximum (Grima, 2000; Grima et al., 2000). Table 5 shows the rotated matrix for the five components given in Table 4 and the factor loadings for each variable after rotation. It can be seen that the rotated table not only shows the loadings of each variable in new components ( $PC_R$ ), but also shows how the variables are separated between columns according to their characteristics or to the properties that they represent. The table shows that the first  $PC_R$  is mostly related to gas content of the mined coalbed with both overburden and rank positively correlated with total and lost plus desorbed gas contents. The highest loading is from total gas content (0.960), followed by lost plus desorbed gas (0.954), rank (0.907), and overburden thickness (0.808). The second  $PC_R$  represents longwall panel dimensions, coal productivity, and underground

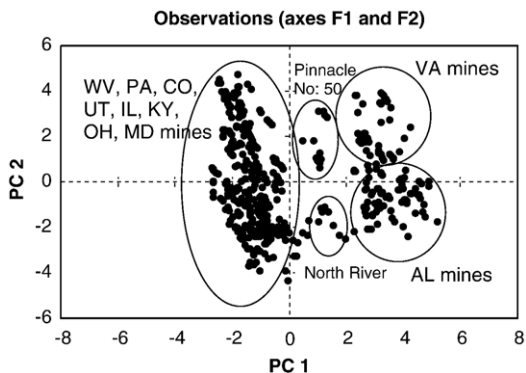


Fig. 7. A two-dimensional distribution of factor scores of each mine (Table 1) on the first two principle components determined by PCA for 1985–2005. The plot shows the groupings of mines of similar characteristics (based on 17 variables).

Table 5  
Factor loadings of the variables after rotating the principle component (PC<sub>R</sub>) matrix using Kaiser's varimax rotation

Variables	PC <sub>R</sub> 1	PC <sub>R</sub> 2	PC <sub>R</sub> 3	PC <sub>R</sub> 4	PC <sub>R</sub> 5
Degasification	0.472	0.221	0.163	0.245	<b>0.538</b>
Basin	-0.287	-0.007	<b>0.917</b>	-0.136	-0.145
State	0.002	0.049	<b>0.951</b>	-0.196	0.002
Seam height	0.064	0.113	-0.093	<b>0.925</b>	-0.063
Cut height	0.048	-0.027	-0.225	<b>0.911</b>	-0.043
Panel width	0.036	<b>0.798</b>	-0.006	0.004	-0.029
Panel length	-0.248	<b>0.701</b>	0.093	-0.202	0.052
Overburden	<b>0.808</b>	-0.075	-0.129	0.108	0.121
Number of entries	0.271	-0.178	-0.045	-0.224	<b>0.805</b>
Cut depth	0.125	<b>0.745</b>	0.056	0.142	-0.076
Face conveyor speed	0.145	<b>0.834</b>	0.116	0.056	-0.167
Stage loader speed	0.147	<b>0.811</b>	-0.048	0.070	0.105
Lost+desorbed gas	<b>0.954</b>	0.024	-0.187	0.065	-0.011
Residual gas	-0.244	0.237	0.748	0.032	0.372
Total gas	<b>0.960</b>	0.077	-0.036	0.076	0.068
Rank	<b>0.907</b>	0.031	-0.174	-0.091	0.186
Coal production	-0.221	<b>0.688</b>	0.251	0.114	0.036

Bold entries show the most influential variables in each PC<sub>R</sub> (Section 3.2).

coal transportation. In this group, face and stage conveyer speeds have the highest loadings (0.834 and 0.811, respectively), followed by longwall panel width, cut depth, and panel length. The loading of coal production is less. However, coal production for a given year is a function of other parameters in this column, such as cut depth and panel dimensions. Therefore, it is incorrect to say that coal production has less importance in determining ventilation emissions.

The third PC<sub>R</sub> in Table 5 is related to the geographical location of the mine determined by state and coal basin. These variables have high loadings in this component, 0.951 and 0.917, respectively. They are the only variables in the database that may be linked to the impacts of underground geology, overlying strata, and reservoir properties of the coalbeds on ventilation emissions. However, since a single coal basin can be present in more than one state, and underground geology may change based on geographical location, the state variable seems to be a better identifier to signify a local area. The fourth PC<sub>R</sub> represents the coalbed and mining height in the longwall environment. These parameters affect potential emissions from the thickness of the fractured strata and the methane emissions from face and ribs. Also, the difference between seam height and cut height may indicate that the unmined portion of the seam is going to be left in the caved zone and that its methane emissions will contribute to the ventilation emissions. The fifth PC<sub>R</sub> represents the ventilation system components. The only parameters that represent

ventilation system components in the database are the number of gateroad entries and the presence or absence of any degasification system. In most cases, if the methane content of the coalbed or strata is high, vertical gob gas ventholes and vertical and horizontal degasification boreholes are drilled to remove gas before it enters the ventilation system (Karacan et al., 2007b).

It should be noted that the groupings of the variables determined by PCA are in accordance with the groupings of the variables used in discussing their effects on emissions (Section 2.2). Since the relationships between most of the parameters and the ventilation emissions are non-linear, the results of PCA need to be evaluated with care. However, it seems reasonable to include input variables from each of the five PCs into the ANN model development in order to capture roughly 80% of variance in the data and to represent those aspects impacting ventilation emissions.

#### 4. Development of ANN for predicting ventilation emissions from longwall mines

##### 4.1. Basic considerations of building an ANN

A neural network simulates a highly interconnected, parallel computational structure of the brain with many relatively simple individual processing elements, called *neurons* (Eberhart and Dobbins, 1990). The input–output flow of a network is determined by the connections and the operation of the neurons. The operation of a single neuron is dependent on the weighted sum of the incoming signals and a bias term, fed through an activation function, resulting in an output. This process can be shown as (Grima, 2000):

$$y_i = f \left( \sum_{r=1}^n w_{ir} f \left( \sum_{j=1}^m v_{rj} u_j + b_r \right) + c_i \right) \quad i = 1, \dots, l \quad (3)$$

where  $u$  is the  $m \times 1$  input vector,  $y$  the  $l \times 1$  output vector,  $n$  the number of neurons in the hidden layer,  $v$  and  $w$  are the weight factors,  $f(\cdot)$  is the activation function, and  $b_r$  and  $c_i$  are the bias values of the neurons in the hidden and output layers. Neurons are networked (topology) in a number of ways depending on the problem type and complexity. One of the most widely used topologies is the multilayer perceptron (MLP) because it can be applied in almost every kind of modeling, general classification, and regression. One of the critical issues in using MLPs is the choice of the number of neurons, and thus weights, in the hidden layers (Hornik et al., 1989; Flood and Kartam, 1994; Maier and Dandy, 2000).

Within the hidden layer, the inputs are summed and processed by a non-linear function, called a transfer function, or axon. While there are various transfer functions, the hyperbolic tangent is generally the preferred transfer function. The non-linear nature of this function plays an important role in the performance of a neural network.

The process of finding a suitable set of weights is called “training.” Training is one of the most important steps in the development of the neural network, since the weights and the network characteristics will be used later in testing data sets and making subsequent predictions. The most common way of training the networks is via the supervised training algorithms, which require repeated showings (epochs) of both input vectors and the expected outputs of the training set to the network to allow it to learn the relations. The number of epochs needed to give an acceptable average error and the initial weights before training are important considerations.

The neural network computes its output at each epoch and compares it with the expected output (*target*) of each input vector in order to calculate the error. An error is defined for a given pattern (input–output) and summed over all output neurons over the entire epoch. Then, the error is summed over all neurons giving a grand total for all neurons and all patterns. Finally, the grand total is divided by the number of patterns to give an average mean squared error (MSE) (Eberhart and Dobbins, 1990). Minimizing this error is the goal of the training process. The most widely used technique is to propagate the error back and adjust the weights in the network, a process called back-propagation.

During error minimization, it is preferable to find the global optimum rather than local optima. This situation is helped by applying a *momentum* factor between 0 and 1. Momentum increases the effective step size in shallow regions of error surface (Hassoun, 1995) and helps speed up the training process.

Once the training phase is complete, the performance of the network needs to be validated on an independent data set. Cross validation is a model evaluation method that gives an indication of how the ANN will perform when it is confronted with data it has not yet seen. It is important that the validation data is not used as part of training (Maier and Dandy, 2000) since this will deteriorate the results of the validation.

#### 4.2. Preliminary models and the search for effective input parameters

Development of an ANN uses parameter estimation and structure identification as fundamental steps. Using

PCA as described in the previous sections gives a good idea as to which input parameters can potentially be included in a longwall ventilation emission model. However, it does not tell how many and exactly which parameters should be included in the model to cope with the complexity, non-linearity, and multivariable nature of the problem. PCA simply reduces the complexity and allows for a more targeted search.

This section presents the results of initial modeling attempts to find the appropriate input parameters for ANN modeling using NeuroSolutions 5.0 (NeuroDimension, 2006). This attempt was undertaken using a heuristic approach. The strategy began with an ANN structure common to all models, where the input parameters were subsequently changed to find the model yielding the best results. For this phase, 10 different models were evaluated. In all models, the training and geometry options were the same. By keeping them so, all models and results had common properties which allowed for suitable comparisons.

For the initial models, a two-hidden layer ANN was constructed with 50 and 30 processing elements for the first and second layers, respectively. A hyperbolic tangent was selected as the transfer function for all layers and a momentum factor of 0.7 was applied for 1500 training epochs. The step size was 1 between the input and first hidden layer and 0.01 between the second hidden and output layer.

Table 6

Different models tested in ANN for their efficiency in predicting ventilation emissions and the variables included

Model number	Input variables*
1	OB, L+D gas, panel W, face C.S., coal P., state, seam H.
2	OB, L+D gas, panel W, face C.S., coal P., state, seam H., panel L.
3	OB, L+D gas, panel W, stage L.S., coal P., state, seam H.
4	OB, total gas, panel W, face C.S., coal P., state, seam H.
5	Total gas, panel W, face C.S., coal P., state, seam H., cut H.
6	Total gas, panel W, face C.S., coal P., state, seam H., cut H., stage L.S.
7	Total gas, panel W, face C.S., coal P., state, seam H., cut H., stage L.S., rank
8	Total gas, panel W, face C.S., coal P., state, seam H., cut H., stage L.S., entries
9	Total gas, panel W, face C.S., coal P., state, seam H., cut H., stage L.S., cut D.
10	Total gas, face C.S., coal P., state, seam H., entries

\* OB: Overburden; L+D gas: lost+desorbed gas; panel w: panel width; face C.S.: face conveyor speed; stage L.S.: stage loader speed; panel L.: panel length; seam H.: seam height; cut H.: cut height; cut D.: cut depth; coal P.: coal production.

Table 7  
Training and cross validation mean squared errors (MSE) for each tested model

Model number	Training MSE	Cross validation MSE
1	0.00652	0.00766
2	0.00562	0.00816
3	0.00721	0.00869
4	0.00651	0.00729
5	0.00701	0.00639
6	0.00533	0.00812
7	0.00621	0.00725
8	0.00670	0.00854
9	0.00529	0.00799
10	0.00867	0.01284

For pre-processing of the data, the whole dataset (exemplars) was first randomized and then separated into three sections for use in the training, cross validation, and testing phases. Randomization was used to prevent the biases and to make different sections of the dataset representative of the whole population. In separating the dataset, 403 out of 538 exemplars (75%) were saved as training data, 54 exemplars (10%) were saved as a cross validation data set, and 81 exemplars (15%) were saved for testing the trained network.

Table 6 summarizes the variables used in the prospective models. In order to evaluate the performance of these models, minimum mean squared errors (MSE) were noted for training and cross validation phases. The values of nominal mean squared error (NMSE), regression coefficient ( $R$ ), and minimum and maximum absolute errors, as well as MSE, were noted for testing.

Tables 7 and 8 show the performances of the models in the training and cross validation phase and in the testing phase, respectively. The data show that almost all models produce low training and cross validation errors. However, testing errors which can be evaluated by MSE, NMSE,  $R$ , and minimum and maximum absolute errors are lower for “model 8” than for the other models. In testing of “model 8,” an MSE of 1.817 and an NMSE of 0.097 with regression coefficient to testing data of 0.95 are achieved.

Table 8  
Performance of the tested models given in Table 6 with “testing” data set

Model number	1	2	3	4	5	6	7	8	9	10
MSE	2.528	2.682	2.582	2.523	1.821	1.968	1.924	1.817	1.971	2.275
NMSE	0.135	0.143	0.137	0.134	0.097	0.105	0.102	0.097	0.105	0.121
Min. error m <sup>3</sup> /day (MMscf/day)	623.04 (0.022)	339.84 (0.012)	453.12 (0.016)	509.76 (0.018)	56.64 (0.002)	84.96 (0.003)	113.28 (0.004)	368.16 (0.013)	28.32 (0.001)	877.92 (0.031)
Max. error m <sup>3</sup> /day ( $\times 10^3$ ) (MMscf/day)	119.31	150.49	129.08	136.50	113.39	100.79	108.81	95.81	131.55	141.66
$R$	4.213	5.314	4.558	4.820	4.004	3.559	3.842	3.383	4.645	5.002
	0.931	0.925	0.931	0.931	0.950	0.946	0.947	0.950	0.946	0.938

Table 9  
Testing performance of the final ANN model using the variables of “model 8” in Table 6 after optimizing network parameters

Performance parameter	
MSE	1.613
NMSE	0.086
Min. error m <sup>3</sup> /day (MMscf/day)	84.96 (0.003)
Max. error m <sup>3</sup> /day ( $\times 10^3$ ) (MMscf/day)	87.42 (3.087)
$R$	0.956

Also, the least maximum absolute error [ $95.8 \times 10^3$  m<sup>3</sup>/day (3.383 MMscf/day)] is achieved with this model. Thus, total gas content, panel width, face conveyor speed, coal production, state, seam height, cut height, stage loader speed, and number of entries were selected as the input variables for the ventilation emission model.

#### 4.3. Determination of final network parameters

After selecting the “model 8” input parameters, the optimum network parameters were searched to improve the predictive performance of the ventilation emission model. For this purpose, various combinations of parameters were tested. The number of hidden layers was chosen as two and the hyperbolic tangent transfer function was used as it was in the base model. The number of processing elements in hidden layers and the value of momentum were varied to improve the model predictions. Values of minimum and final mean squared error (MSE) were noted for training and cross validation of the ANN. Also, values of nominal mean squared error (NMSE), regression coefficient, and absolute error were noted for testing the ANN.

First, the numbers of processing elements in the first hidden layer were varied between 44 and 62, while keeping the number of processing elements in the second layer at 30, keeping momentum at 0.7, and running the network for 1500 epochs. The results showed that 56 processing elements in the first hidden

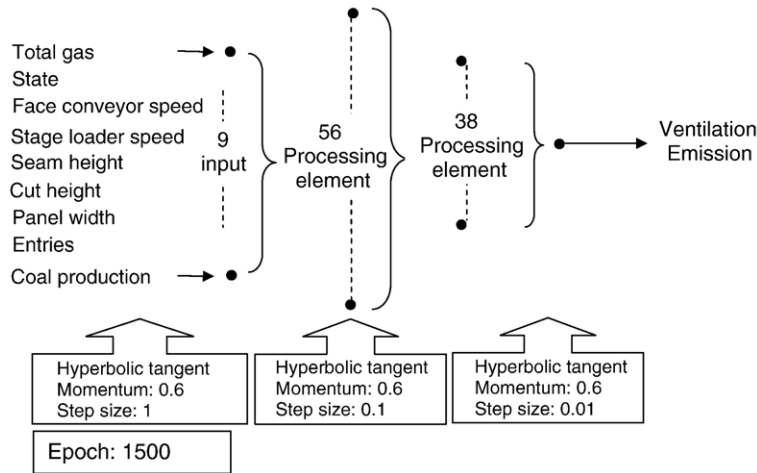


Fig. 8. The inputs, topology and the parameters of the proposed ANN model for predicting ventilation methane emissions from longwall mines.

layer produced the best MSE values of 0.00456 and 0.00823 for training and cross validation, respectively.

Next, the processing elements in the second hidden layer were varied between 26 and 40, while setting the number of processing elements in the first hidden layer to 56. The results showed that 38 processing elements in the second hidden layer produced minimum MSEs of 0.00460 and 0.00660 for training and cross validation, respectively.

Finally, the momentum value was varied between 0.5 and 0.8 while setting the first and second hidden layer processing elements to 56 and 38, respectively. The best MSE values of 0.00501 and 0.00719 were achieved for training and cross validation, respectively, using a momentum value of 0.6. Table 9 shows the performance parameters of this network with the testing data set. Optimization of the number of processing elements in the hidden layers and the momentum value improved the

performance of the network in the face of new data. Table 9 shows that MSE and NMSE values improved from 1.817 to 1.613 and from 0.097 to 0.086, respectively. The minimum and maximum absolute errors decreased to  $7.6 \times 10^{-5}$  m<sup>3</sup>/day (0.003 MMscf/day) and to  $87.4 \times 10^3$  m<sup>3</sup>/day (3.087 MMscf/day), respectively. Similarly, *R* improved from 0.95 to approximately 0.96. Fig. 8 shows the topology and parameters of the final ANN network proposed for predicting longwall ventilation emissions.

Fig. 9 compares the target emission rates in the test data set with the predicted values using the model in Fig. 8. The comparison of the target data with the predicted values in Fig. 9 shows that the performance of the network in predicting emissions is reasonably good despite the large variations in the data. This comparison also indicates the flexibility and interpolation/extrapolation performance of the network.

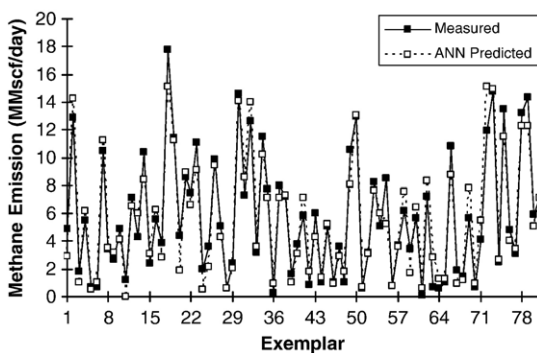


Fig. 9. Comparison of target methane emission rates (measured values in the database) of the “testing” data set with the predicted rates from the proposed ANN shown in Fig. 8 (1 MMscf=28,320 m<sup>3</sup>).

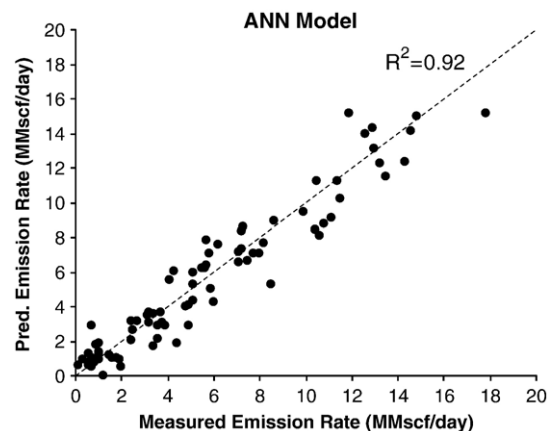


Fig. 10. A scatter plot of measured methane emissions and ANN predictions of the “testing” data set (1 MMscf=28,320 m<sup>3</sup>).

## 5. Comparison of ANN predictions with statistical models

In this section, the predictive capability of the ANN model shown in Fig. 9 is compared with multilinear and second-order non-linear statistical models. For this purpose, two statistical models having the same input variables as the ANN model were developed. These models were developed using the training data used to “train” the ANN network. However, predictive capabilities of the statistical models were tested using the “test” data used to evaluate the performance of ANN. This approach enabled all the models to be developed and compared on the same basis. The linear and non-linear models are shown in Eqs. (4) and (5), respectively.

$$\text{Emission} = a_0 + a_1V_1 + a_2V_2 + \dots + a_9V_9 \quad (4)$$

$$\text{Emission} = a_0 + a_1V_1 + a_2V_2 + \dots + a_9V_9 + b_1V_1^2 + b_2V_2^2 \dots + b_9V_9^2 \quad (5)$$

In these equations,  $V_n$  are the variables ( $n=1$  to  $9$ ),  $a_n$  values are the coefficients of first degree variables, and  $b_n$  values are the coefficients of second degree variables.

Figs. 10–12 show the plots of measured emissions versus predicted values using the ANN, linear, and non-linear models, respectively. Fig. 10 shows that the ANN model is capable of predicting the test data reasonably well ( $R^2=0.92$ ). The linear model (Fig. 11) and even non-linear model (Fig. 12), on the other hand, are less successful in predicting the new data using the same variables. The  $R^2$  values in these cases are 0.54 and 0.61 for linear and non-linear models, respectively. These

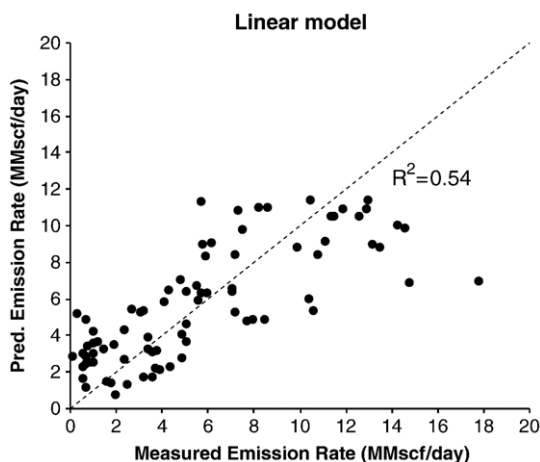


Fig. 11. A scatter plot of measured methane emissions and multilinear model Eq. (4) predictions of the “testing” data set (1 MMscf=28,320 m<sup>3</sup>).

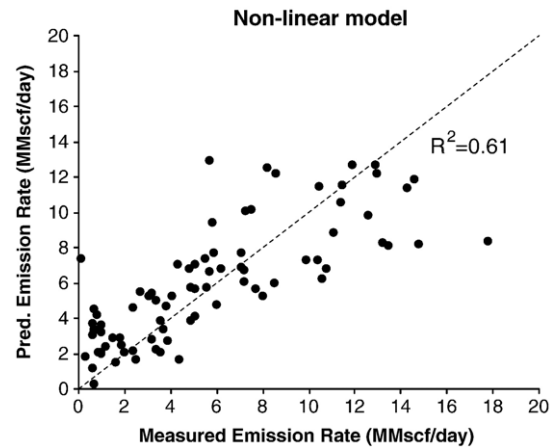


Fig. 12. A scatter plot of measured methane emissions and second-order non-linear model Eqn. (5) predictions of the “testing” data set (1 MMscf=28,320 m<sup>3</sup>).

data show that the ANN model is superior when compared to the statistical models in predicting ventilation emissions from longwall mines. This is due to the highly non-linear and variable nature of the data, for which the ANN demonstrates more flexibility in capturing trends and making generalizations compared to other models.

## 6. Summary and conclusions

Prediction of ventilation methane emissions from longwall mines is complex due to the various factors contributing to these emissions. There are few mathematical models in the literature that can be used to predict methane emissions from longwall mines. The objective of this work was to develop an artificial neural network (ANN)-based model for the prediction of ventilation methane emissions from U.S. longwall operations.

Ventilation methane emission data obtained from 63 U.S. longwall mines in 10 states were combined with corresponding coalbed properties, geographical information, longwall operation parameters, and coal productions for the years 1985–2005. The variables in the dataset were analyzed with principle component analysis (PCA) to determine their impacts on methane emissions. A number of models were tested to find the best combination of variables for the prediction of ventilation emissions using the ANN approach. Finally, the parameters of the ANN were optimized and the predictive performance was compared with linear and non-linear models.

The results of the above process showed that ventilation emissions could be defined by a number of variables, each representing a particular emission contributor. In this study, PCA and preliminary test models

showed that state, total gas content of coalbed, seam and cut heights, panel width, face conveyor speed, stage loader speed, number of entries, and coal productions were the most effective parameters to predict ventilation emissions. The ANN algorithm yielded good results for predicting emissions. A two-hidden layer model with 56 and 38 processing elements in each layer was found to be sufficient. Also, 1500 epochs were enough to train the network for satisfactory results.

Comparison of the ANN model with the linear and non-linear statistical models showed that the ANN model performed better using the testing data due to its flexibility and highly non-linear nature. A regression coefficient of 0.92 was obtained from the ANN as compared to 0.54 and 0.61 for linear and non-linear models, respectively.

The presented approach using PCA and ANN is one of the more accurate models to predict methane emissions from longwall mines. By incorporating the critical stratigraphic features in place of geographical information, the approach and the model can be applied to other mines.

## Acknowledgements

Barbora Jemelkova of the U.S. Environmental Protection Agency is thanked for her help in obtaining ventilation methane emission data. W.P. Diamond is thanked for his help in obtaining gas content data.

## References

- Addinsoft, 2007. *Xlstat-Pro user's manual*. New York, NY.
- Bagherieh, A.H., Hower, J.C., Bagherieh, A.R., Jorjani, E., in press. Studies of the relationship between petrography and grindability for Kentucky coals using artificial neural network. *International Journal of Coal Geology*.
- Bibler, C., Marshall, J., Pilcher, R.C., 1998. Status of worldwide coal mine methane emissions and use. *International Journal of Coal Geology* 35, 283–310.
- Boyer, C.M., Qingzhao, B., 1998. Methodology of coalbed methane resource assessment. *International Journal of Coal Geology* 35, 349–368.
- Davis, J.C., 1986. *Statistics and Data Analysis in Geology*, 2nd edition. Wiley and Sons, New York.
- Diamond, W.P., 1994. Methane control for underground coal mines. US Bureau of Mines Information Circular No. 9395. Pittsburgh, PA.
- Diamond, W.P., Schatzel, S.J., 1998. Measuring the gas content of coal: a review. *International Journal of Coal Geology* 35, 311–331.
- Diamond, W.P., La Scola, J.C., Hyman, D.M., 1986. Results of direct-method determination of the gas content of the US coalbeds. US Bureau of Mines Information Circular No. 9067. Pittsburgh, PA.
- Eberhart, R.C., Dobbins, R.W., 1990. *Neural Network PC Tools: A Practical Guide*. Academic Press Inc., San Diego, CA.
- Faraway, J., Chatfield, C., 1998. Time series forecasting with neural networks: a comparative study using airline data. *Applied Statistics* 47, 231–250.
- Flood, I., Kartam, N., 1994. Neural networks in civil engineering. I: principles and understanding. *Journal of Computing in Civil Engineering* 8, 131–148.
- Grima, M.A., 2000. *Neuro-fuzzy Modeling in Engineering Geology*. A.A. Balkema, Rotterdam, The Netherlands. 244 pp.
- Grima, M.A., Bruines, P.A., Verhoef, P.N.W., 2000. Modeling tunnel boring machine performance by neuron-fuzzy methods. *Tunneling and Underground Space Technology* 15, 259–269.
- Hassoun, M.H., 1995. *Fundamentals of Artificial Neural Networks*. MIT Press, Cambridge.
- Hornik, K., Stinchcombe, M., White, H., 1989. Multilayer feedforward networks are universal approximators. *Neural Networks* 2, 359–366.
- Karacan, C.Ö., in press. Development and application of reservoir models and artificial neural networks for optimizing ventilation air requirements in development mining of coal seams. *International Journal of Coal Geology*.
- Karacan, C.Ö., Diamond, W.P., 2006. Forecasting gas emissions for coal mine safety applications. In: Kissell, F. (Ed.), *Handbook for Methane Control in Mining*. NIOSH, Information Circular No: 9486, Pittsburgh, PA.
- Karacan, C.Ö., Diamond, W.P., Esterhuizen, G.S., Schatzel, S.J., 2005. Numerical analysis of the impact of longwall panel width on methane emissions and performance of gob gas ventholes. *International Coalbed Methane Symposium, Paper 0505*, Tuscaloosa, Alabama.
- Karacan, C.Ö., Esterhuizen, G.S., Schatzel, S.J., Diamond, W.P., 2007a. Reservoir simulation-based modeling for characterizing longwall methane emissions and gob gas venthole production. *International Journal of Coal Geology* 71, 225–245.
- Karacan, C.Ö., Diamond, W.P., Schatzel, S.J., 2007b. Numerical analysis of the influence of in-seam horizontal methane drainage boreholes on longwall face emission rates. *International Journal of Coal Geology* 72, 15–32.
- Kim, A.G., 1977. Estimating methane content of the bituminous coalbeds from adsorption data. US Bureau of Mines Report of Investigations No. 8245. US Bureau of Mines, Pittsburgh, PA.
- Krog, R.B., Schatzel, S.J., Garcia, F., Marshall, J.K., 2006. Predicting methane emissions from wider longwall panels by analysis of emission contributors. *Proceedings of 11th U.S./North American Mine Ventilation Symposium*, pp. 383–392.
- Lunarzewski, L., 1998. Gas emission prediction and recovery in underground coal mines. *International Journal of Coal Geology* 35, 117–145.
- Maier, H.R., Dandy, G.C., 2000. Neural networks for the prediction and forecasting of water resources variables: a review of modeling issues and applications. *Environmental Modeling and Software* 15, 101–124.
- Mining Media Inc. Coal Age. [http://www.mining-media.com/publications/coal\\_age.asp](http://www.mining-media.com/publications/coal_age.asp).
- US Environmental Protection Agency, 1994. Identifying opportunities for methane recovery at U.S. coal mines: draft profiles of selected gassy underground coal mines. Report No: EPA 430-R-94-012. Washington, D.C.
- US Environmental Protection Agency, 1997. Identifying opportunities for methane recovery at U.S. coal mines: draft profiles of selected gassy underground coal mines. Report No: EPA 430-R-93-012. Washington, D.C.
- US Environmental Protection Agency, 2005. Identifying opportunities for methane recovery at U.S. coal mines: profiles of selected gassy underground coal mines 1999–2003. Report No: EPA 430-K-04-003. Washington, D.C.
- US Mine Safety and Health Administration, 2007. <http://www.msha.gov/drs/drshome.htm>.

- Mucho, T.P., Diamond, W.P., Garcia, F., Byars, J.D., Cario, S.L., 2000. Implications of recent NIOSH tracer gas studies on bleeder and gob gas ventilation design. Proc. Annual Meeting of Society for Mining, Metallurgy and Exploration, Salt Lake City, UT.
- NeuroDimension, 2006. NeuroSolutions 5.0. Gainesville, FL.
- Noack, K., 1998. Control of gas emissions in underground coal mines. *International Journal of Coal Geology* 35, 57–82.
- Palchik, V., 2003. Formation of fractured zones in overburden due to longwall mining. *Environmental Geology* 44, 28–38.
- Pashin, J., 1998. Stratigraphy and structure of coalbed methane reservoirs in the United States: an overview. *International Journal of Coal Geology* 35, 209–240.
- Patel, S.U., Kumar, B.J., Badhe, Y.P., Sharma, B.K., Sha, S., Biswas, S., Chaudhury, A., Tambe, S.S., Kulkarni, B.D., 2007. Estimation of gross calorific value of coals using artificial neural networks. *Fuel* 86, 334–344.
- Peng, S.S., 2006. Longwall mining, Second edition. Morgantown, WV. 621 pp.
- Schatzel, S.J., Krog, R.B., Garcia, F., Marshall, J.K., 2006. Prediction of longwall methane emissions and associated consequences of increasing longwall face lengths: a case study in the Pittsburgh Coalbed. Proceedings of 11th U.S./North American Mine Ventilation Symposium, pp. 375–382.
- Singh, M.M., Kendorski, F.S., 1981. Strata disturbance prediction for mining beneath surface water and waste impoundments. Proc. 1st Conference on Ground Control in Mining, Morgantown, WV.
- Sousa, S.I.V., Martins, F.G., Alvim-Ferraz, M.C.M., Pereira, M.C., 2007. Multiple linear regression and artificial neural networks based on principle components to predict ozone concentrations. *Environmental Modeling and Software* 22, 97–103.
- Steidl, P., 1996. Chapter 2: coal as a reservoir. In: Saulsberry, J.L., Scahfer, P.S., Schraufnagel, R.A. (Eds.), *Coalbed Methane Reservoir Engineering*. Gas Research Institute, Chicago, IL.
- Thakur, P.C., Poundstone, W.N., 1980. Horizontal drilling technology for advance degasification. *Mining Engineering* 676–680 June.
- Tomita, S., Deguchi, G., Matsuyama, S., Li, H., Kawahara, H., 2003. Development of a simulation program to predict gas emission based on 3D stress analysis. 30th International Conference of Safety in Mines Research Institutes, South African Institute of Mining and Metallurgy, pp. 69–76.
- Ünver, B., Yasıtlı, N.E., 2006. Modeling of strata movement with special reference to caving mechanism in thick coal seam mining. *International Journal of Coal Geology* 66, 227–252.
- Yılmaz, S., Demircioğlu, C., Akın, S., 2002. Application of artificial neural networks to optimum bit selection. *Computers & Geosciences* 28, 261–269.